Progression of Ocular Melanoma Metastasis to the Liver:

The 2012 Zimmerman Lecture

Hans E. Grossniklaus, MD

Departments of Ophthalmology and Pathology, and L. F. Montgomery Laboratory, Emory Eye Center, Emory, University School of Medicine, Atlanta, Georgia

Abstract

Importance—To the best of my knowledge, this study demonstrates for the first time small, apparently dormant micrometastasis in the liver of patients with uveal melanoma.

Objective—To evaluate the histological and immunohistochemical findings in metastatic uveal melanoma to the liver.

Design—Samples of liver were obtained at autopsy from patients who died of metastatic uveal melanoma to the liver.

Setting—L. F. Montgomery Laboratory, Emory Eye Center, Atlanta, Georgia.

Participants—A total of 10 patients who died of metastatic uveal melanoma to the liver.

Intervention—Sections of the liver were examined with hematoxylin-eosin, periodic acid–Schiff, Masson trichrome, or reticulin stains.

Main Outcome Measures—The tumors' morphology, growth pattern, mean vascular density, and mitotic index were determined with the aid of immunohistochemical stains for S100, HMB45, CD31, and Ki67.

Results—Stage 1 metastases (defined as tumor clusters 50 μm in diameter) were identified in the sinusoidal spaces of 9 of 10 patients (90%). Stage 1 metastases were avascular and lacked mitotic activity. Stage 2 metastases (defined as tumors measuring 51–500 μm in diameter) and stage 3 metastases (defined as tumors measuring >500 μm in diameter) were found in all patients. Immunohistochemical stains were positive for S100 or HMB45 in all tumors. Overall, stage 1 metastases outnumbered stage 2 metastases (which outnumbered stage 3 metastases). The mean vascular density and mitotic index increased from stage 2 to stage 3 metastases (*P*<.05). The

Correspondence: Hans E. Grossniklaus MD, L. F. Montgomery Laboratory, Emory Eye Center, BT428, 1365 Clifton Rd, Atlanta, GA 30322 (ophtheg@emory.edu).

architecture of stage 2 metastases mimicked the surrounding hepatic parenchyma, whereas stage 3 metastases exhibited either lobular or portal growth patterns.

Conclusions—Uveal melanoma that spreads to the liver can be categorized as stage 1 (50 μm in diameter), stage 2 (51–500 μm in diameter), or stage 3 (>500 μm in diameter) metastases. The later stage exhibits a lobular or portal pattern of growth. During this progression, tumors become vascularized and mitotically active.

Uveal melanoma, the most common primary intraocular tumor,[1–4] has an associated approximate 40% risk of metastasizing to the liver within 10 years of diagnosis of the primary tumor.[1] Hepatic metastases, which occur in 95% of patients with metastatic uveal melanoma,[5] result in death in almost all cases.[6,7] It is important to understand the pathology of metastatic uveal melanoma to the liver in order to develop rational treatment protocols.

In the late 1970s, Zimmerman and coworkers[8] hypothesized that the enucleation of an eye containing uveal melanoma was a risk factor for the spread of melanoma cells. The cornerstone of their hypothesis was that there was a 2-year postenucleation risk of death for patients with uveal melanoma.[9] Although the hypothesis was rigorously debated, Zimmerman et al[8] emphasized how little was understood about the spread of melanoma beyond the eye. Their hypothesis raised questions about the timing of the hematogenous spread of uveal melanoma and the possibility of tumor dormancy in the liver. After calculating tumor doubling times and extrapolating,[10,11] investigators theorized that clinically undetectable metastatic tumors (micrometastases) exist in the liver at the time of the diagnosis of the primary tumor in patients who go on to develop metastases. Until now, these theoretically dormant micrometastases have not been demonstrated in the livers of patients who have succumbed to metastatic uveal melanoma.

In a single study[12] of postmortem liver tissue samples obtained from patients with uveal melanoma, tumors 200 to 2000 μm in diameter were found in patients who died of metastases, and, in one instance, a single collection of 1 to 3 melanoma cells was found in the liver of a patient who died of a myocardial infarction. In the present study, I examined postmortem hepatic biopsy specimens obtained from 10 patients who succumbed to liver metastases of uveal melanoma in order to assess the histologic growth patterns, immunohistochemical features, vascularity, and mitotic rates of the tumors.

METHODS

The present study was approved by the Emory University School of Medicine institutional review board in Atlanta, Georgia. Ten sections of the livers of patients who died of hepatic metastases from uveal melanoma that had been submitted to the L. F. Montgomery Laboratory, Emory Eye Center, in Atlanta, Georgia, were examined (courtesy of Ian McLean, MD, April 2000). No personal or medical histories were available for the cases other than that they were from adults older than 20 years of age who died of hepatic metastasis from uveal melanoma. Each patient died within 1 to 5 years after the ocular tumor had been treated by enucleation or brachytherapy. There were 10 formalin-fixed, paraffin-embedded, 7-μm–thick unstained slides available for each patient. The sections measured from 7×12 mm to 30×15 mm, with an average of 15×17 mm. The sections were

stained with hematoxylin-eosin (2 slides), periodic acid– Schiff, Masson trichrome, and reticulin stains. Immunohistochemical staining, using the avidin-biotin complex technique (DAKO) with a vector red chromagen, was performed for S100 (1:800) and HMB45 (1:50), both melanoma markers, and using a diaminobenzamine chromagen for smooth muscle actin (1:160) for myofibroblasts, CD31 (1:180) for vascular endothelium, and Ki67 (1:160) as a nuclear proliferation marker. All antibodies were from DAKO, and appropriate positive and negative controls were performed.

To determine the mean vascular density, tumors stained with CD31 were scanned at low magnification (×5; Olympus BHTU) to find the areas in the tumors with the highest vascular density. These areas were then examined with a 40× objective (Olympus), and the number of CD31-positive blood vessels within the tumors were counted and averaged per 5 high-power fields (40× objective). To determine the proliferation rate, 40 high-power fields were examined per tumor, and the percentage of Ki67-positive tumor cells was determined. The mitotic index was determined by counting the number of mitoses in hematoxylin-eosin stains of 40 high-power fields per tumor. There were 2 sections per cases evaluated for counting metastases and 1 section per case for each of the immunohistochemical stains. All metastases were counted and evaluated by the immunohistochemical stains. Measurements of the mean vascular density, the proliferation rate, and the mitotic index were all performed in triplicate and then averaged. The data were statistically analyzed by analysis of variance (GraphPad Prism, http://www.graphpad.com/scientific-software/prism), and $P<.05$ was defined as statistically significant.

RESULTS

A histological examination showed that all sections contained metastatic melanoma. Aggregates of melanoma cells were identified in the sinusoidal spaces in 9 of the 10 patients. By estimating the number of cells on serial sections, I found that there were approximately 10 to 100 melanoma cells per aggregate, and the aggregates measured from 10 to 50 μm in diameter. The aggregates were designated as stage 1 metastases. Individual melanoma cells were occasionally found in the vicinity of the aggregates. The nuclei of these small collections of tumor cells contained bland, evenly dispersed chromatin. Stage 1 metastases were easily identified with immunohistochemical stains for HMB45 (Figure 1).

In some cases, the stage 1 metastases had expanded within the sinusoidal spaces and formed large clusters that measured 51 to 500 μm in diameter. These outgrowths were designated as stage 2 metastases. A distinguishing feature of stage 2 metastases was that the intervening hepatocytes had disappeared. Stage 2 metastases were often inconspicuous and blended with the surrounding hepatic parenchyma. Reticulin stains demonstrated pseudosinusoidal spaces within stage 2 metastases that mimicked the surrounding hepatic parenchyma, although these metastases could be better visualized with an HMB45 stain (Figure 2). The pseudosinusoidal spaces in the stage 2 metastases were lined by smooth muscle actin–positive activated stellate cells (myofibroblasts).

Metastases that measured greater than 500 μm in diameter were designated as stage 3 metastases and displayed 2 patterns of growth. The first pattern infiltrated and replaced the

hepatic lobules with associated perilobular septal fibrosis and were highlighted with a trichrome stain. Only small islands of intact hepatocytes remained in these tumors. This pattern of growth was termed "lobular." The second pattern consisted of large islands of tumor cells adjacent to portal venules that effaced rather than infiltrated liver parenchyma. These tumors, which contained numerous CD31-positive vascular channels and areas of necrosis, were designated as exhibiting a "portal" growth pattern (Figure 3).

Immunohistochemical stains were strongly positive for HMB45 in 9 of 10 patients and for S100 in 2 of 10 patients, including 1 patients whose sample was negative for HMB45. Immunohistochemical stains were positive in all stages of metastases. Stage 1 outnumbered stage 2 (which outnumbered stage 3 metastases in all cases) (Figure 4; eTable 1, http://www.jamaophth.com). All stage 1 metastases were entirely avascular, but stage 2 metastases contained occasional CD31-positive vascular channels, whereas stage 3 metastases contained many CD31-positive vascular channels (Figure 5; eTable 2). A minimum of 100 tumor cells in each stage were examined to determine Ki67 positivity and the proliferation rate. Evaluation of the proliferation rate showed that stage 1 metastases contained less than 1%, stage 2 contained 1% to 5%, and stage 3 contained 5% to 10% of tumor cells that were positive for Ki67, respectively. Similarly, the mitotic index increased from stage 1 to stage 2 to stage 3 metastases (Figure 6; eTable 3). Of note, none of the stage 1 metastases contained mitotic figures.

COMMENT

Uveal melanoma, with rare exception, metastasizes hematogenously. Primary tumor cells that express high levels of c-Met invade the vasculature of uveal melanoma where they gain access to the general circulation.[13] Circulating melanoma cells respond to a chemotactic gradient of stroma-cell–derived factor through CXCR4 and home to the liver.[14–17] There is experimental evidence that, once in the liver, individual melanoma cells give rise to micrometastases.[18–20] There is further experimental evidence that tumors have the capacity to remain dormant. Dormancy in this context refers to a state in which many tumor cells are in the G0 phase of the cell cycle, and the proliferative rate of those cells not in G0 is offset by the rate of apoptosis.[21] There is also evidence that an angiogenic switch controls the transition from avascular micrometastases to vascularized metastases.[21,22] The inference from the present study is that human livers that contain metastatic uveal melanoma avascular stage 1 metastases appear to progress through stage 2 to larger stage 3 metastases that exhibit vascularization and proliferative activity in either a portal or lobular growth pattern (Figure 7).

The progression of hepatic metastases other than uveal melanoma, such as colon carcinoma, provides insight and puts the present study into context.[23] A proposed mechanism of progression of hepatic metastases of uveal melanoma is as follows. In the liver, metastatic tumor cells are filtered through the sinusoidal space. Here, lodged tumor cells induce proinflammatory factors that regulate cell adhesion to the sinusoidal endothelium.[23] For instance, IL-18 produced by the sinusoidal endothelium induces tumor and endothelial production of hydrogen peroxide, which in turn promotes tumor-endothelial cell adhesion

and vascular endothelial growth factor–dependent tumor cell proliferation.[23] These collections of melanoma cells are now stage 1 metastases.

Simultaneously, hepatic stellate cells are activated and become smooth muscle actin–positive myofibroblasts. These transformed stellate cells invade the metastatic tumor and provide a scaffold for tumor growth prior to the development of new vessels (ie, angiogenesis).[23] The hypothesis based on the histologic findings is that the stage 2 metastases identified in the present study appear to have arisen from expansions of clusters of stage 1 metastases. The stage 2 metastases contained pseudosinusoidal spaces lined by stellate cell–derived smooth muscle actin–positive myofibroblasts. This space may represent an expanded compartment between the sinusoidal endothelium and hepatocytes (space of Disse). Stage 2 metastases appeared to receive nutrition and oxygen via the intercalary canal system provided by these pseudosinusoidal spaces. Furthermore, stage 2 metastases were camouflaged as they mimicked the architecture of the surrounding hepatic parenchyma. This architectural similarity may explain the difficulty that exists in detecting incipient growth clinically. As the tumors grew, they either replaced the hepatic lobule (lobular growth pattern) or, when present adjacent to a portal venule, effaced and pushed the surrounding hepatic parenchyma aside (portal growth pattern). These growth patterns may be related to the first occurrence of the tumor in the lobule in the former or adjacent to a terminal branch of the portal vein in the latter.[23] There is no temporal progression from the lobular to portal or portal to lobular growth pattern implied. The aforementioned proposed progression needs to be validated.

There are similarities and differences between the present study and the only previous study[12] of the his tological features of metastatic uveal melanoma to the liver. The prior study[12] found a collection of 1 to 3 melanoma cells in the liver in 1 of 6 patients with uveal melanoma who died of nonmelanoma causes. Metastatic melanomas that measured 200 to 2000 μm in diameter were found in the livers of 16 patients who died of metastatic uveal melanoma.[12] The prior study[12] used a panmelanoma immunohistochemical antibody, whereas, in the present study, I used S100 and HMB45. In the present study, HMB45 was strongly positive in 9 of 10 patients, and S100 was positive in 2 of 10 patients, with HMB45 being more sensitive than S100 for detecting all stages of the melanomas in the liver. Stage 1 and stage 2 metastases may be inconspicuous on hematoxylin-eosin stains and may become apparent with immunohisto-chemical staining for HMB45. Both the previous study[12] and the present study showed a conspicuous absence of inflammatory cells in the liver associated with the melanoma metastases. Although the present study could not evaluate individual metastatic melanoma cell survival in the liver, the previous autopsy study[12] and experimental models indicate that few melanoma cells can survive in the liver for prolonged periods to spawn metastases.[24] The establishment of melanoma cells in the liver is likely a stochastic phenomenon that is related to tumor burden and the mechanical properties of cells lodging in sinusoidal spaces.

There is evidence that end-organ control, in this case the liver, is involved with limiting the progression of metastatic tumor cells. Clinical[25] and experimental[26] studies have shown that the innate immune system (in particular, natural killer cells residing in the liver and known as "pit" cells) eliminates metastatic uveal melanoma cells that fail to express HLA class I

antigen. There is also some evidence that aged, polarized macrophages in the hepatic microenvironment contribute to metastatic uveal melanoma progression.[27] My laboratory now has experimental evidence that liver production of pigment epithelium–derived factor controls micrometastatic melanoma progression to metastases (H. E. Grossniklaus, MD, H. Yang, MD, PhD, and S. Crawford, DO, unpublished data, 2010). Pigment epithelium–derived factor is a substrate for matrix metalloproteinases types 2 and 9.[28] Matrix metalloproteinases types 2 and 9 are produced by tumor cells and trigger the angiogenic switch during carcinogenesis.[29] It is likely that melanoma cell production of matrix metalloproteinases in the liver eventually degrades the liver's pigment epithelium–derived factor, thus allowing micrometastatic tumor progression (including angiogenesis). These phenomena could not be investigated in the present study owing to limited tissue availability.

The major weakness of this study is the lack of demographic data (including clinical histories), which obviates any temporal correlation of events, including laboratory studies. Demographic data may likely explain differences in results between this study and the previous autopsy study.[12] Another weakness is that there was limited tissue available to evaluate for the role of the immune response, pigment epithelium–derived factor, and matrix metalloproteinases with regard to metastatic melanoma progression. These studies will be performed as more tissue becomes available. The present study provides a framework for future evaluation of hepatic metastatic uveal melanoma.

The findings in the present study show that, importantly, subclinical stage 1 metastases are present in the livers of patients with metastatic uveal melanoma. These small tumors exhibit signs of dormancy, including bland nuclear cytologic features and an absence of mitotic activity. As tumors progress and enlarge, they become vascularized, and mitotic activity is demonstrable. Such findings suggest that the liver controls tumor progression, including changes in innate immunity, macrophage aging, and pigment epithelium–derived factor degradation. The hypothesis generated from the present study is that the Zimmerman et al[8] effect of increased clinically detectable metastases peaking at approximately 2 years after treatment of the primary uveal melanoma is the result of a stochastic phenomenon of tumor burden and the loss of end-organ tumor suppression. Further experimentation and pathologic evaluation should eventually prove or disprove this hypothesis.

Acknowledgments

References

1. Singh AD, Shields CL, Shields JA. Prognostic factors in uveal melanoma. Melanoma Res. 2001; 11(3):255–263. [PubMed: 11468514]

2. Singh AD, Topham A. Incidence of uveal melanoma in the United States: 1973–1997. Ophthalmology. 2003; 110(5):956–961. [PubMed: 12750097]

3. Stang A, Jöckel KH. Trends in the incidence of ocular melanoma in the United States, 1974–1998. Cancer Causes Control. 2004; 15(1):95–96. author reply 101–102. [PubMed: 15049325]

4. Burr JM, Mitry E, Rachet B, Coleman MP. Survival from uveal melanoma in England and Wales 1986 to 2001. Ophthalmic Epidemiol. 2007; 14(1):3–8. [PubMed: 17365812]

5. Collaborative Ocular Melanoma Study Group. Assessment of metastatic disease status at death in 435 patients with large choroidal melanoma in the Collaborative Ocular Melanoma Study (COMS): COMS report no. 15. Arch Ophthalmol. 2001; 119(5):670–676. [PubMed: 11346394]

6. Bedikian AY. Metastatic uveal melanoma therapy: current options. Int Ophthalmol Clin. 2006; 46(1):151–166. [PubMed: 16365561]

7. Augsburger JJ, Corrêa ZM, Shaikh AH. Effectiveness of treatments for metastatic uveal melanoma. Am J Ophthalmol. 2009; 148(1):119–127. [PubMed: 19375060]

8. Zimmerman LE, McLean IW, Foster WD. Does enucleation of the eye containing a malignant melanoma prevent or accelerate the dissemination of tumour cells. Br J Ophthalmol. 1978; 62(6): 420–425. [PubMed: 352389]

9. Singh AD, Rennie IG, Kivela T, Seregard S, Grossniklaus H. The Zimmerman-McLean-Foster hypothesis: 25 years later. Br J Ophthalmol. 2004; 88(7):962–967. [PubMed: 15205248]

10. Eskelin S, Pyrhönen S, Summanen P, Hahka-Kemppinen M, Kivelä T. Tumor doubling times in metastatic malignant melanoma of the uvea: tumor progression before and after treatment. Ophthalmology. 2000; 107(8):1443–1449. [PubMed: 10919885]

11. Singh AD. Uveal melanoma: implications of tumor doubling time. Ophthalmology. 2001; 108(5): 829–831. [PubMed: 11319992]

12. Borthwick NJ, Thombs J, Polak M, et al. The biology of micrometastases from uveal melanoma. J Clin Pathol. 2011; 64(8):666–671. [PubMed: 21593344]

13. Hendrix MJ, Seftor EA, Seftor RE, et al. Regulation of uveal melanoma interconverted phenotype by hepatocyte growth factor/scatter factor (HGF/SF). Am J Pathol. 1998; 152(4):855–863. [PubMed: 9546344]

14. Li H, Alizadeh H, Niederkorn JY. Differential expression of chemokine receptors on uveal melanoma cells and their metastases. Invest Ophthalmol Vis Sci. 2008; 49(2):636–643. [PubMed: 18235009]

15. Bakalian S, Marshall JC, Logan P, et al. Molecular pathways mediating liver metastasis in patients with uveal melanoma. Clin Cancer Res. 2008; 14(4):951–956. [PubMed: 18281525]

16. All-Ericsson C, Girnita L, Seregard S, Bartolazzi A, Jager MJ, Larsson O. Insulin-like growth factor-1 receptor in uveal melanoma: a predictor for metastatic disease and a potential therapeutic target. Invest Ophthalmol Vis Sci. 2002; 43(1):1–8. [PubMed: 11773005]

17. Haider, HKh; Jiang, S.; Idris, NM.; Ashraf, M. IGF-1-overexpressing mesenchymal stem cells accelerate bone marrow stem cell mobilization via paracrine activation of SDF-1alpha/CXCR4 signaling to promote myocardial repair. Circ Res. 2008; 103(11):1300–1308. [PubMed: 18948617]

18. Diaz CE, Rusciano D, Dithmar S, Grossniklaus HE. B16LS9 melanoma cells spread to the liver from the murine ocular posterior compartment (PC). Curr Eye Res. 1999; 18(2):125–129. [PubMed: 10223656]

19. Logan PT, Fernandes BF, Di Cesare S, Marshall JC, Maloney SC, Burnier MN Jr. Single-cell tumor dormancy model of uveal melanoma. Clin Exp Metastasis. 2008; 25(5):509–516. [PubMed: 18335317]

20. Yang H, Fang G, Huang X, Yu J, Hsieh CL, Grossniklaus HE. In-vivo xenograft murine human uveal melanoma model develops hepatic micrometastases. Melanoma Res. 2008; 18(2):95–103. [PubMed: 18337645]

21. Udagawa T, Fernandez A, Achilles EG, Folkman J, D'Amato RJ. Persistence of microscopic human cancers in mice: alterations in the angiogenic balance accompanies loss of tumor dormancy. FASEB J. 2002; 16(11):1361–1370. [PubMed: 12205027]

22. Yang H, Jager MJ, Grossniklaus HE. Bevacizumab suppression of establishment of micrometastases in experimental ocular melanoma. Invest Ophthalmol Vis Sci. 2010; 51(6):2835–2842. [PubMed: 20089875]

23. Vidal-Vanaclocha F. The prometastatic microenvironment of the liver. Cancer Microenviron. 2008; 1(1):113–129. [PubMed: 19308690]

24. Luzzi KJ, MacDonald IC, Schmidt EE, et al. Multistep nature of metastatic inefficiency: dormancy of solitary cells after successful extravasation and limited survival of early micrometastases. Am J Pathol. 1998; 153(3):865–873. [PubMed: 9736035]

25. Blom DJ, Luyten GP, Mooy C, Kerkvliet S, Zwinderman AH, Jager MJ. Human leukocyte antigen class I expression: marker of poor prognosis in uveal melanoma. Invest Ophthalmol Vis Sci. 1997; 38(9):1865–1872. [PubMed: 9286277]

26. Yang H, Dithmar S, Grossniklaus HE. Interferon alpha 2b decreases hepatic micrometastasis in a murine model of ocular melanoma by activation of intrinsic hepatic natural killer cells. Invest Ophthalmol Vis Sci. 2004; 45(7):2056–2064. [PubMed: 15223777]

27. Herwig MC, Grossniklaus HE. Role of macrophages in uveal melanoma. Expert Rev Ophthalmol. 2011; 6(4):405–407. [PubMed: 22003361]

28. Notari L, Miller A, Martínez A, et al. Pigment epithelium-derived factor is a substrate for matrix metalloproteinase type 2 and type 9: implications for downregulation in hypoxia. Invest Ophthalmol Vis Sci. 2005; 46(8):2736–2747. [PubMed: 16043845]

29. Bergers G, Brekken R, McMahon G, et al. Matrix metalloproteinase-9 triggers the angiogenic switch during carcinogenesis. Nat Cell Biol. 2000; 2(10):737–744. [PubMed: 11025665]
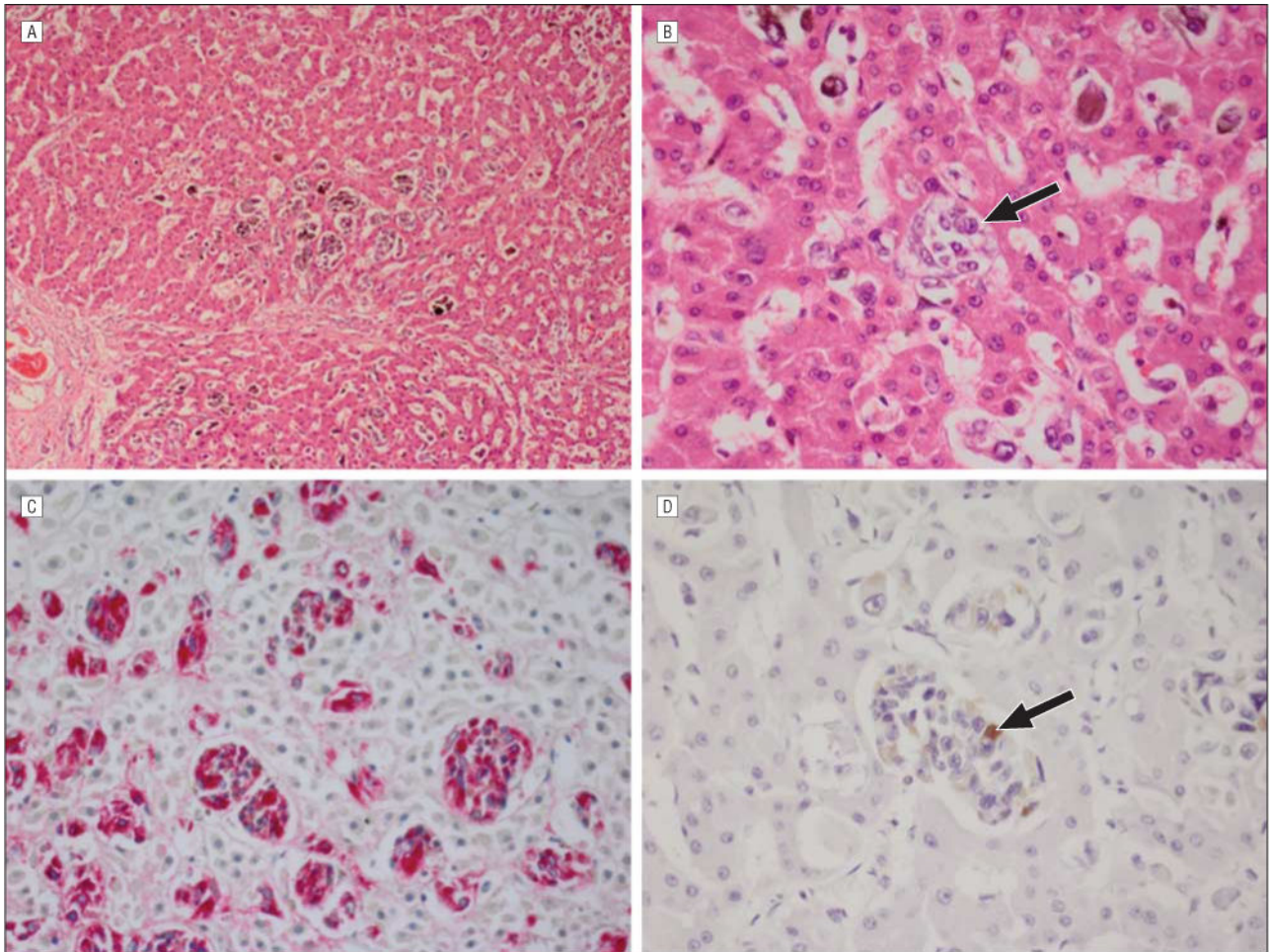
Figure 1.
Stage 1 metastatic uveal melanoma. A, There are scattered stage 1 metastases arranged in clusters in the liver parenchyma (hematoxylin-eosin, original magnification ×25). B, An individual stage 1 metastasis (arrow) is present in a sinusoidal space (hematoxylin-eosin, original magnification ×100). C, Immunohistochemical staining for HMB45 (red reaction product) clearly highlights the stage 1 metastases (avidin-biotin complex with vector red chromagen, original magnification ×100). D, Immunohistochemical staining for Ki67, a proliferation marker, is positive (arrow) in less than 1% of nuclei in stage 1 metastases (avidin-biotin complex with diaminobenzedine chromagen, original magnification ×100).
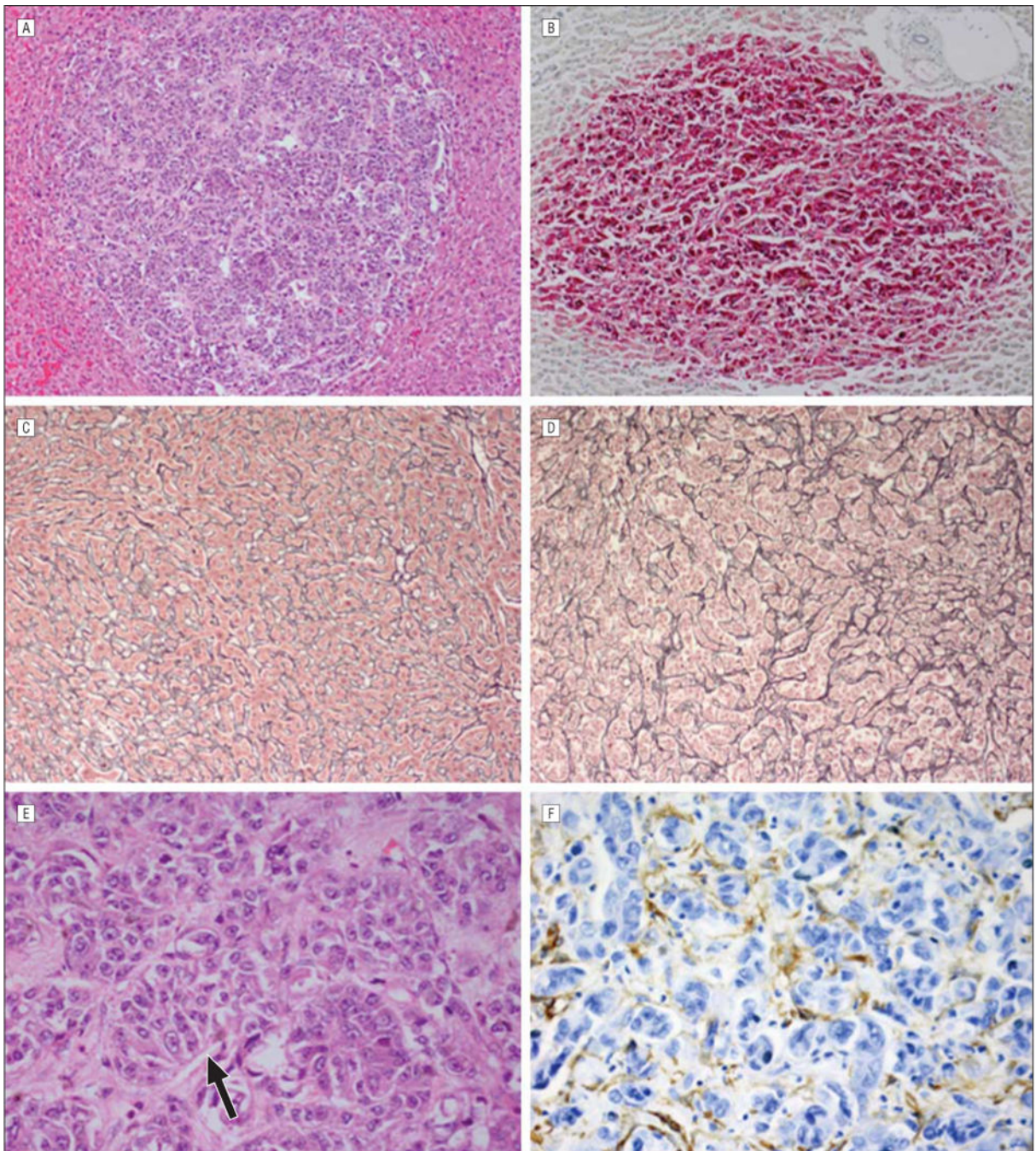
Figure 2.
Stage 2 metastatic uveal melanoma. A, A focal stage 2 uveal melanoma metastasis is present in the liver parenchyma (hematoxylin-eosin, original magnification ×25). B, Immunostaining for HMB45 is strongly positive in the melanoma cells (avidin-biotin complex with vector red chromagen, original magnification ×25). C, The sinusoidal spaces are lined with type 3 collagen highlighted with a reticulin stain in normal liver (original magnification ×25). D, There are pseudosinusoidal spaces in the stage 2 metastasis that are also lined with reticulin-positive type 3 collagen (original magnification ×25). E, Higher

magnification demonstrates the pseudosinusoidal spaces (arrow) in the stage 2 metastases (hematoxylin-eosin, original magnification ×100). The hepatocytes have been destroyed. F, Immunohistochemical stains are positive for smooth muscle actin in activated stellate cells (myofibroblasts) lining the pseudosinusoidal spaces (avidin-biotin complex with diaminobenzedine chromagen, original magnification ×100).
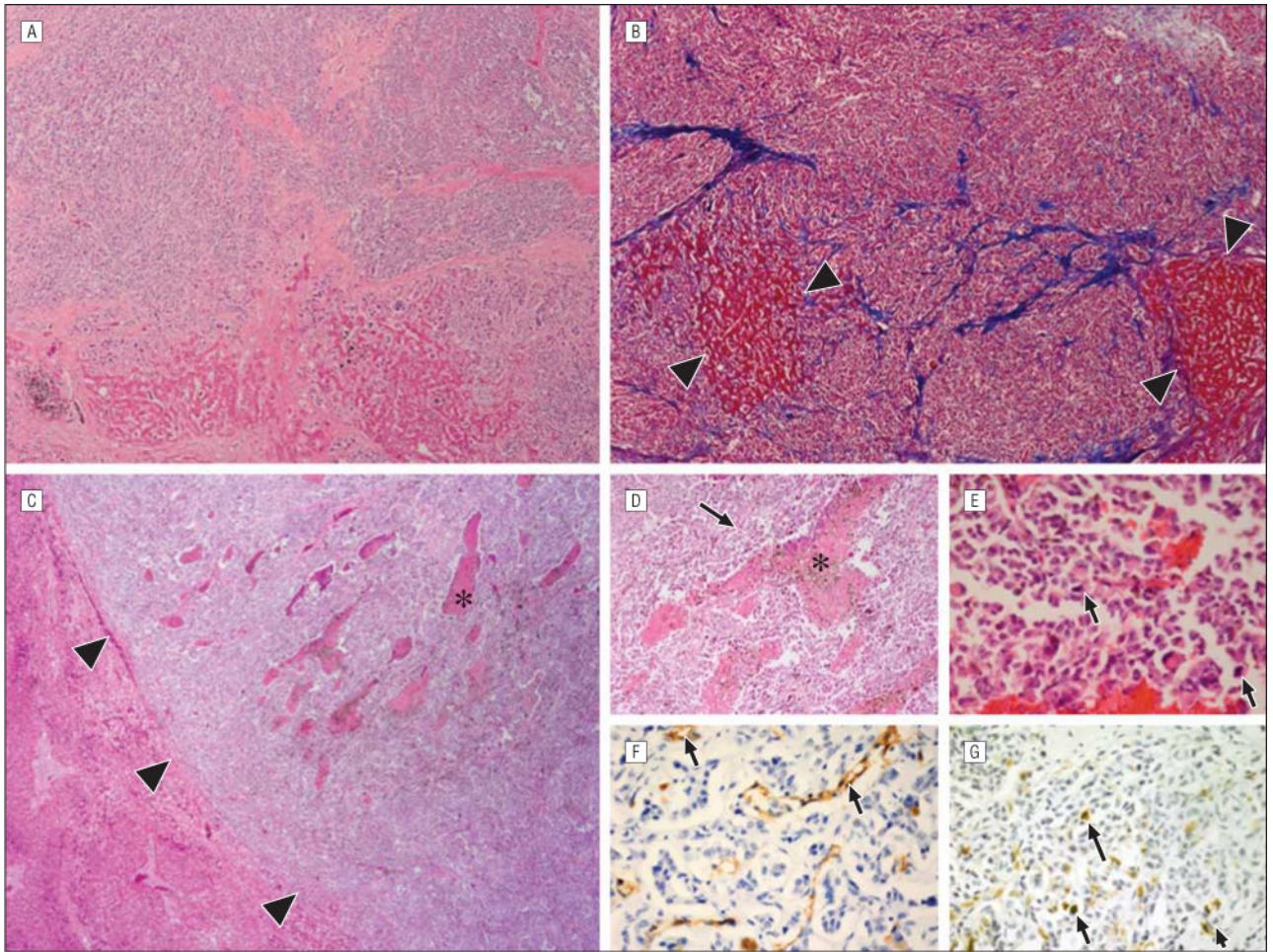
Figure 3.
Stage 3 metastatic uveal melanoma. A and B, The lobular growth patterns of metastases are shown (hematoxylin-eosin, original magnification ×10 [A]; Masson trichrome, original magnification ×10 [B]). The melanoma has expanded within the portal lobule and infiltrated the liver. Only small islands of hepatic parenchyma remain (between the arrowheads). The lobules are outlined by thick collagen bands that stain blue with a trichrome stain. C, The portal growth pattern of metastasis contains areas of necrosis (asterisk) and effaces or pushes aside the surrounding liver parenchyma (hematoxylin-eosin, original magnification ×10). The interface between a single large metastasis and a normal surrounding liver is demarcated with arrowheads. Higher magnification of a single stage 3 metastasis shows areas of necrosis and neovascularization (D [asterisk and arrow]; hematoxylin-eosin, original magnification ×100), mitotic figures (E [arrows]; hematoxylin-eosin, original magnification ×100), CD31-positive vascular channels (F [arrows]; avidin-biotin complex with diaminobenzedine chromagen, original magnification ×100), and Ki67-positive nuclei (G [arrows]; avidin-biotin complex with diaminobenzedine chromagen, original magnification ×100).
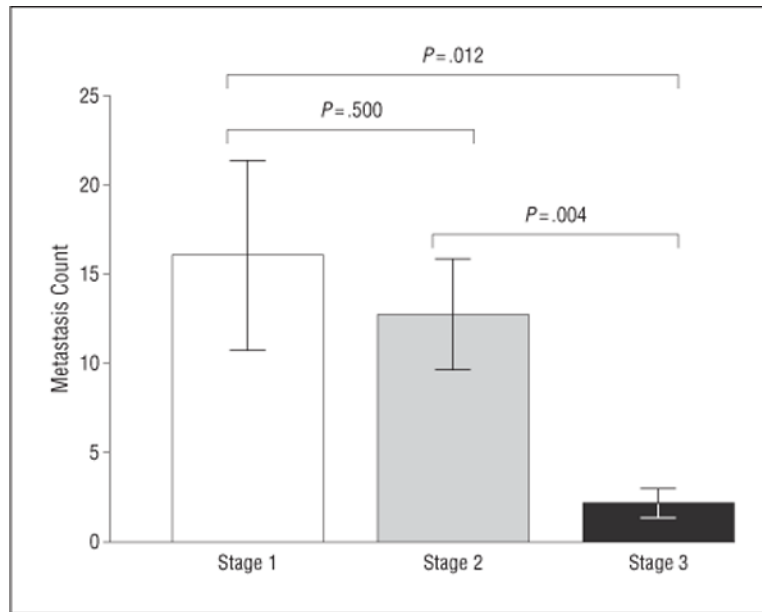
Figure 4.
Numbers of stage 1 metastases, stage 2 metastases, and stage 3 metastases per section (ie, the metastasis count). There were significantly more stage 1 metastases than stage 2 metastases, and there were significantly more stage 2 metastases than stage 3 metastases, in all cases. Error bars represent 1 SEM.
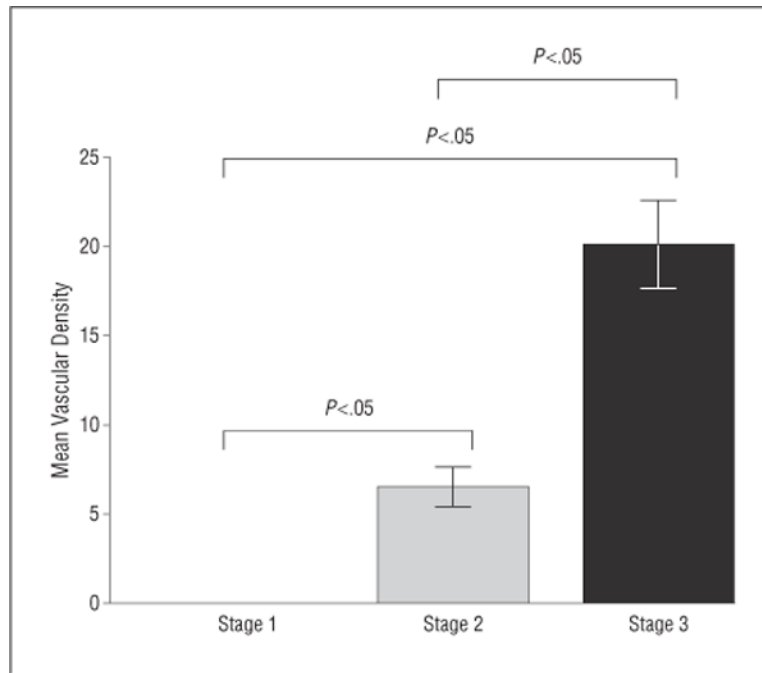
Figure 5.
Mean vascular density in stage 1, stage 2, and stage 3 metastases. There were no blood vessels identified in stage 1 metastases. The mean vascular density significantly increased from stage 2 to stage 3 metastases. Error bars represent 1 SEM.
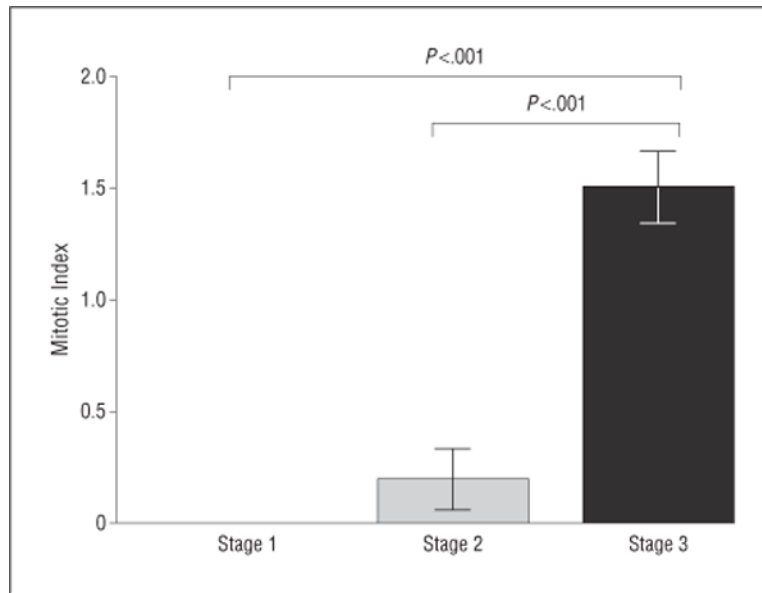
Figure 6.
Mitotic indexes of stage 1, stage 2, and stage 3 metastases. There were no mitotic figures in stage 1 metastases. There was a significant increase in the mitotic index in stage 2 and stage 3 metastases. Error bars represent 1 SEM.
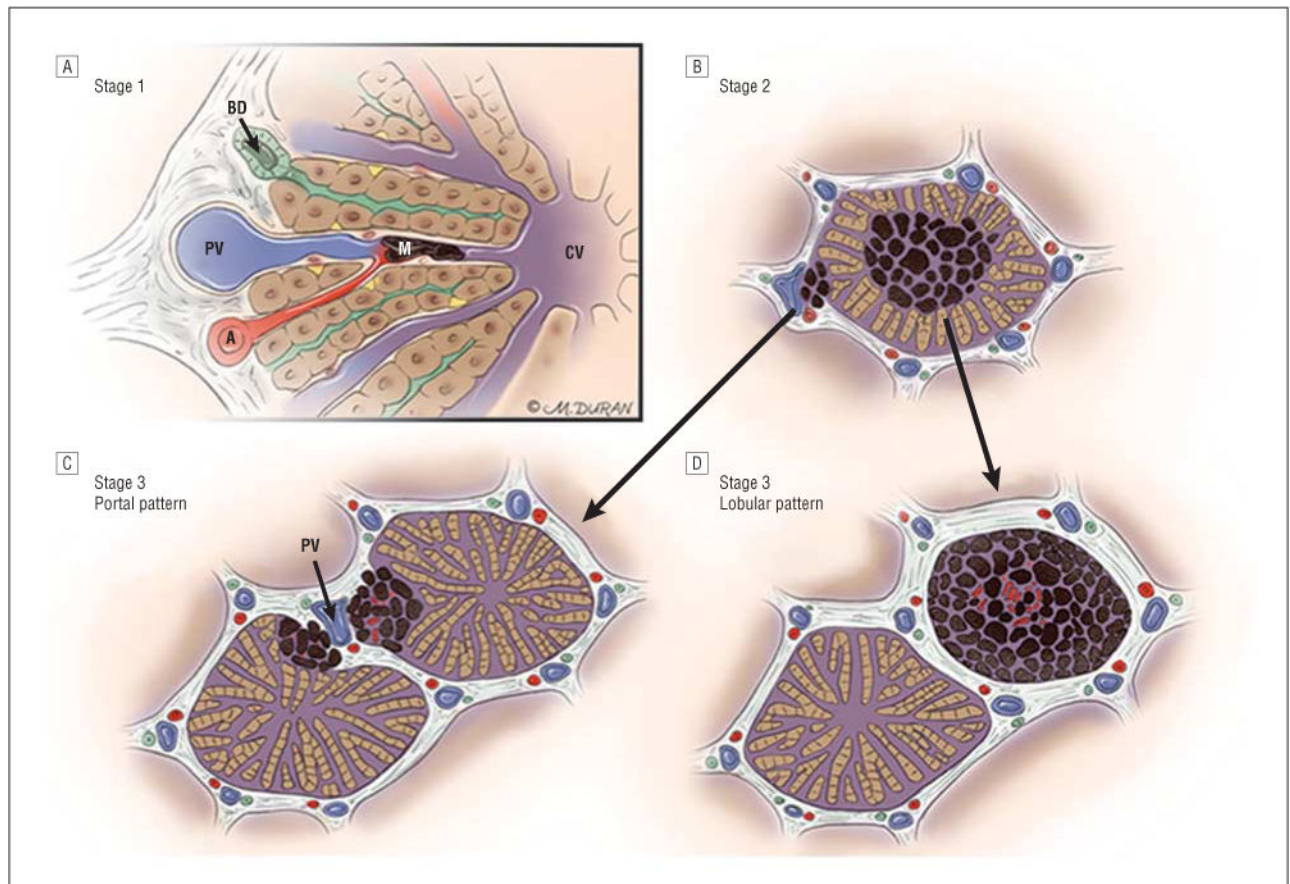
Figure 7.
Progression of ocular melanoma metastasis to the liver through stages 1, 2, and 3. A, In stage 1, up to 50 μm in diameter of avascular aggregates of melanoma (M) arise in sinusoidal spaces via the hepatic arteriole (A); blood flows in the sinusoidal space from the hepatic arteriole and portal venule (PV) toward the central vein (CV); bile flows in the opposite direction toward a bile ductule (BD). B, In stage 2, aggregates of melanoma coalesce to form 51 to 500 μm in diameter of metastases and co-opt the portal venule or infiltrate the hepatic lobule with loss of hepatocytes, proliferation of stellate cells, and the appearance of pseudosinusoidal spaces. C, In stage 3, metastases that measure greater than 500 μm in diameter may grow in a portal pattern in which they co-opt the portal venule (PV). D, Metastases may also infiltrate the hepatic lobule in the lobular pattern.